

MODELING HUMAN ARM MOVEMENTS CONSTRAINED BY ROBOTIC SYSTEMS

Karin Hollerbach¹ and H. Kazerooni²
Department of Mechanical Engineering
University of California, Berkeley
Berkeley, California

ABSTRACT

The human arm in constrained movements, is in continuous contact with its environment. The defining characteristic of the human arm in such movements is associated with the ability of the human to impose desired forces. Examples of constrained movements can be seen in telerobotic systems, orthotic devices, and robotic systems worn by humans (Kazerooni 1991). We describe a theoretical and experimental analysis for constrained movements of the human arm.

NOMENCLATURE

α	feedback parameter representing the bandwidth of the human central nervous system
B	viscosity in G_m
C	DC feedback gain
f_h	the contact force imposed on the environment by the human arm
f_i	the intended force applied by the muscles, as commanded by the central nervous system
G_a	operator describing muscle activation dynamics
G_{cns}	operator relating neural input to the muscles and the arm configuration, p
G_i	operator mapping the position constraint, p , into the contact force, f_h
G_f	feedback operator whose output affects the descending neural signals, n
G_m	operator representing the inertial and viscoelastic properties of the muscles and passive tissues surrounding the joint
K	stiffness in G_m
M	inertia in G_m
n	descending neural input to the muscles
p	arm configuration

1. INTRODUCTION

Fundamental differences in human arm behavior can be related to two types of movements: constrained and unconstrained. In constrained movements, the human arm moves in such a way that the environment continuously exerts a dynamic constraint on the arm. The "environment", in this instance, is the object that is in continuous contact with the human arm. In unconstrained movements, the arm moves in its workspace without contact with the environment and, therefore, without contact forces between the arm and the environment. Examples of constrained movements can be seen when the arm is moving an exercise machine or is constrained by an orthotic device. In systems of this nature, the human arm dynamics are integrated with the machine dynamics, resulting in behavior specific to the total system. Therefore, the performance and stability of the system taken as a whole are both functions of not only the machine dynamics, but also the human arm dynamics. Instability of machines that interact with humans has been reported in (Kazerooni 1990). In this article, we examine the dynamics of constrained movements of the human arm, where the environment dictates the position, while the human maintains a desired contact force.

In contrast to our work, previous studies have focused on posture maintenance, disturbance rejection, and trajectory tracking in the presence of disturbing sinusoidal, trapezoidal, and pulse forces. (Berthoz and Metral 1970) examined the dynamic behavior of the human elbow in response to external forces applied at the forearm, while the subject maintained visual control of the forearm position. In this study, the ratio of the displacement to the amplitude of the imposed sinusoidal force (admittance) was measured at various frequencies. A maximum value for the admittance was observed in the range of 3-5 Hz with a noticeable reduction above 6

¹ Ph.D. Candidate in Bioengineering Graduate Group

² Associate Professor in Mechanical Engineering Department

Hz. In 1950, Wilkie concluded that "rigidity" of a limb is increased by simultaneous contraction of antagonist muscles; this results in a smaller joint admittance and more effective posture maintenance. This conclusion was confirmed by Murray and Hogan (1989), who determined that deliberate co-contraction of antagonist muscles is an effective means of rejecting torque disturbances to maintain posture. Furthermore, Murray and Hogan demonstrated that co-contraction is, in fact, used for this purpose in able-bodied persons. Winters and Stark (1985) provided further evidence for the influence of co-contraction on limb response to external loading (force disturbance rejection) in human single joint motion. In this study, a lumped parameter, antagonist muscle model was employed to simulate a variety of movement trajectories from isometric to fast ballistic motions. A high co-contraction level was observed to cause a strong resistance in low frequency forces by raising both model stiffness and viscosity. In an antagonist muscle model of the human wrist, Agarwal et al. (1970) studied the behavior of the human wrist in response to pulse torque disturbances. They reported changes in stiffness and viscosity by factors of 10 and 70, respectively, with varying levels of co-contraction.

We are interested in the behavior of the arm as it interacts continuously with an environment that imposes a position constraint on the arm, while the human can only attempt to regulate the contact force. This work can be considered dual to the studies listed above. The duality may be seen in the experimental methods: Instead of applying a disturbance force and measuring the resultant movement, as was done in previous studies, we apply a continuous position constraint and measure the resultant contact forces between the source of the perturbation and the arm. Experiments of this nature will lead to an understanding of force maintenance and position disturbance rejection. For example, Crowninshield et al. (1976) studied differences between intact and injured human knees in an effort to develop a clinically useful method for assessing ligamentous injury. In doing so, they carried out a set of experiments in which they imposed position constraints on the knee and reported the ratio of the knee force to the imposed position. Throughout this article, this ratio will be referred to as the "impedance".

In this article, we arrive at a model that adequately describes a range of human elbow behavior in constrained motions. The dynamic modeling presented here is necessary to design controllers for active machines that interact with human arms. Section 2 is dedicated to a dynamic model of the human arm. We use an input-output model, as the detailed dynamic behavior of the arm muscles is of less concern in this study and is implicitly accounted for in the model. Section 3 describes a set of experiments to verify the theory. The experiment employs a computer controlled, active machine that imposes a position constraint on the human arm. This machine is instrumented with force sensors and encoders for measuring human arm forces and positions.

2. DYNAMIC MODEL

We model constrained, single joint movements of the human arm. As a specific example, the joint being modeled may be the elbow joint, actuated by the elbow flexor (biceps) and the elbow extensor (triceps). We avoid attributing a particular class of dynamic behaviors to constrained movements of the human arm, as it is not clear whether the arm behaves as a force or a position control system in constrained motions. Maneuvering our hands in a stream of water from one point to another target point, while struggling with the water current, is an example that shows the human arm can work as a position control in a constrained space and can continuously accept a position or velocity command from the central nervous system. Alternatively, pushing a pin into a wall is an example of a constrained movement where the human imposes a force on the pin, without being concerned with the pin position in the direction normal to the wall; this system may be viewed as one that accepts force commands from the central nervous system. Considering the above dilemma in attributing a particular control action to constrained movements of the human arm, we use a Norton or a Thevenin equivalent concept (Senturia and Wedlock 1975) to arrive at a general substitute for the dynamic behavior of the human arm interacting with the environment. In the same way that the choice of a Norton or Thevenin equivalent does not affect the behavior of a circuit in contact with other circuits, our choice in modeling the human arm by a Norton or a Thevenin equivalent has no effect on the arm's interaction with other systems.

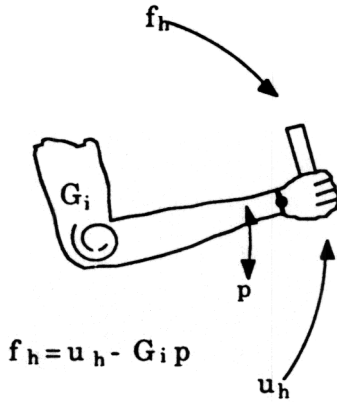
Using the "force-current" analogy between electrical and mechanical systems, a Norton equivalent is now chosen to model the human arm's dynamic behavior as a non-ideal source of force interacting with other systems. The notion of "non-ideal", as applied here, refers to the fact that the arm responds not only to descending commands from the central nervous system but also to position constraints imposed by interaction with the environment. u_h is that part of the contact force that is imposed by the muscles, as commanded by the central nervous system (Figure 1). If the arm does not move (i.e. the arm position, $p = 0$), the total contact force, f_h , is the same as u_h . However, f_h is also a function of the environmental position constraint. If the arm moves, (i.e. the environment imposes a position constraint on the arm), the force imposed on the environment will differ from u_h . The analogy can be observed from the Norton equivalent circuit shown in Figure 1(c): The current, f_h , is a function of not only the current source, u_h , but also the external voltage, p . Considering the above analogy, shown in Figure 1, the contact force, f_h , can be represented by equation (1):

$$f_h = u_h - G_i p \quad (1)$$

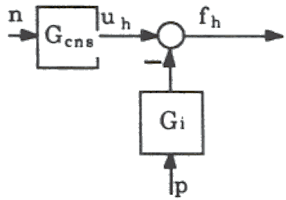
Throughout this article, G_i is referred to as the human arm impedance and maps the environmental position constraint into the contact force.

Here we give a brief description of the internal structure of the human arm impedance, G_i , using Figure 2. Figure 2 consists of three elements:

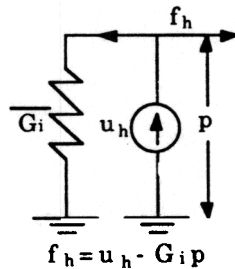
1. **Muscle Activation Dynamics.** G_a , produces an intended muscle force, f_i , in response to descending neural commands, n .
2. **Muscular Contraction and Passive Tissue Dynamics.** G_m represents the properties of the muscles and the passive tissues surrounding the joint, and reduces the intended force by $G_m p$.
3. **Neural Feedback.** G_f is a feedback operator regulating the force imposed by human arm on the environment.



(a)



(b)



(c)

Figure 1: (a) In constrained movements, the contact force, f_h , is a function of not only the commands, n , from the central nervous system but also of the imposed position constraint, p . (c) represents the Norton equivalent circuit of the dynamics shown in (b). The current, f_h , is a function of not only the current source, n , but also of the imposed voltage drop, p .

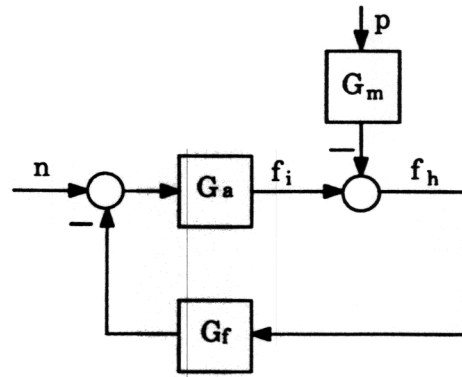


Figure 2: The internal structure of Figure 1 (b) is presented, where the neural feedback mechanism, G_f , allows for regulation of the contact force, f_h .

The following is the brief discussion of the three features listed above:

Muscle Activation Dynamics.

G_a represents muscle activation dynamics and maps the descending neural control signals into the intended muscle force, f_i (Zahalak 1990). We rely on this model, since this type of model for muscle activation dynamics has been used with some success in other work (Zajac 1989). Decoupled operators³ for muscle activation dynamics are generally used with Hill-type muscle models (Winters 1990). We are interested, however, in the overall behavior of the arm and wish to suppress the details of muscle behavior. Thus, G_a is the only operator we use that explicitly describes muscle behavior. A first order time lag has been suggested in (Zajac 1989) to represent G_a .

Muscular Contraction and Passive Tissue Dynamics

G_m is an impedance that reduces the intended force, resulting in the total contact force, f_h . G_m implicitly takes into account both the internal muscle dynamics, such as the force-velocity and length-tension relationships (Rack and Westbury 1984, Wilkie 1950, Hill 1970), and the changing effective stiffness of the arm that results from varying the co-contraction of the antagonistic muscles; G_m also includes the dynamic behavior of the passive tissues surrounding the joint. Equation (2) describes G_m .

$$G_m = M s^2 + B s + K \quad (2)$$

where M represents the mass of the human arm, and K and B define the visco-elastic behavior of the muscles and passive tissues.

Note that in the human arm, the descending neural control signals have two functions: (1) causing the arm to move, and (2) altering the arm impedance, G_m . Here, we model the first of these functions by n in

³ Use of a decoupled operator for the activation dynamics implies that muscular activation is assumed to be independent of the muscular contraction process.

Figure 2. The second function, altering the arm impedance, is not explicitly shown but is accounted for in G_m . See Humphrey and Reed (1983) for more information on neurophysiological evidence for the existence of two separate cortical systems, one for determining the commanded limb trajectory, the other for specifying the level of co-contraction.

Neural Feedback

The interaction force, f_h , exerted by the arm on its environment is used as a feedback signal to modulate the descending neural signals. This feedback is effective only at relatively low frequencies because of the limited bandwidth of the central nervous system. Since the human hand is able to very accurately apply a desired interaction force at very low frequencies, we deduce that G_f is very large at low frequencies. (The experimental results, discussed in Section 3, will clarify this.) On the other hand, since the human cannot apply a desired interaction force at high frequencies, G_f must be very small in the high frequency range. Assuming G_f as a linear transfer function, equation (3) is an appropriate choice

$$G_f = \frac{C}{s + \alpha} \quad (3)$$

where α is a small number representing the bandwidth of the central nervous system, and C is a feedback gain. In addition, one may introduce a pure time delay operator in order to account for neural conduction delay.

Simplifying the block diagram shown in Figure 2 results in the transfer functions shown in Figure 1.

$$f_i = G_{cns} n + G_i p \quad (4)$$

where

$$G_{cns} = \frac{G_a}{1 + G_f G_a} \quad (5)$$

$$G_i = \frac{G_m}{1 + G_f G_a} \quad (6)$$

G_{cns} and G_i , represent, respectively, the effect of the central nervous system commands and of the interaction force, f_h . These operators are shown in Figure 1 (b). Note that Figure 1(b) mathematically represents the concepts of Figure 2: The force imposed by the human arm on the environment is the result of both the central nervous system commands and the environmental position constraint.

A comparison of our modeling approach with that of Wieneke and Denier van der Gon (1974) leads to the duality described in Section 1. In their modeling approach, an interaction force was modeled as the imposed disturbance, while the resultant position was modeled as the feedback variable. In contrast, in our modeling approach, the interaction force is modeled as the feedback variable, while the position is modeled as the imposed disturbance

3. EXPERIMENTAL METHODS AND RESULTS

In this section, we provide preliminary experimental evidence in support of the model that we have presented.

In order to relate the experimental evidence to the model, we note that the measured force between the robot handle and the human hand is represented by the contact force, f_h , in the model.

Several experiments have been conducted to measure the human arm impedance represented in the model by G_i . In the experiments, the subject grabbed the robot shown in Figure 3. The robot was commanded to oscillate via small-amplitude sinusoids of known frequency in the sagittal plane (parallel to the plane of symmetry in the human body) along the y direction shown in Figure 3.

At each oscillation frequency of the robot, the human operator attempted to follow the robot so that zero contact force was maintained between his hand and the robot. Two experiments were conducted at two different co-contraction levels. In the first experiment, the subject maintained a relatively loose grip on the robot handle. The contact force, f_h , and position, p , were measured at each oscillation frequency. The ratio of f_h to p , at each frequency, represents G_i and is shown in Figure 4. In the second experiment, the subject grabbed the handle with a relatively tight grip. Figure 5 shows the results of the second experiment.

In comparing the data in the two figures, we observe that the human arm impedance at low co-contraction levels (Figure 4) is significantly smaller than it is at high co-contraction levels (Figure 5) in the low frequency range. These results are hardly surprising, given the evidence discussed above that both stiffness and viscosity are roughly proportional to mean muscle tension and that co-contraction has an especially strong influence on both parameters at low frequencies (Winters and Stark 1985).

At high frequencies, the forearm is moved without the benefit of the active feedback loop, G_f . In the high frequency region, we observe that the impedance behaves like a purely inertial load in both plots. These data agree with previous results (Lehman and Calhoun 1990, Wieneke et al. 1974), in which passive wrist motion was shown to be second order and dominated by the moment of inertia.

From the curve fitted to the experimental data depicted in Figures 4 and 5, we obtain the theoretical impedance calculation:

$$G_i = 0.143 s^2 + 1 s + 2.51 \quad \text{lb/ft} \quad (\text{for Figure 4}) \quad (7)$$

$$G_i = 0.277 s^2 + 2.38 s + 12.1 \quad \text{lb/ft} \quad (\text{for Figure 5}) \quad (8)$$

Cross over frequencies in experimental G_i of 3-6 rad/sec were observed. The cross over frequency is the

maximum frequency at which the subject was able to accurately control the constrained movement, for a given co-contraction level. The cross over frequency creates the distinction between the low and the high frequency regions of operation and is itself defined by the time delays associated with finite neural conduction velocities.

In the experiments described here, the human elbow joint was made to operate solely within the mid-portion of its full range of motion. Thus, we avoided significant non-linearities associated with joint torques caused by passive tissues around the joint. Lehman and Calhoun (1990) determined that passive elastic torques in the human wrist are small and relatively constant within 40 degrees in either direction from the middle of the wrist's range of motion, and rise rapidly at either extreme of the full range of motion. Similar results were observed by Hayes and Hatze (1977) in the human elbow joint. Moreover, the passive viscous torque was found to vary by a factor of approximately 5, with an obvious minimum at a point within the mid-range of the joint.

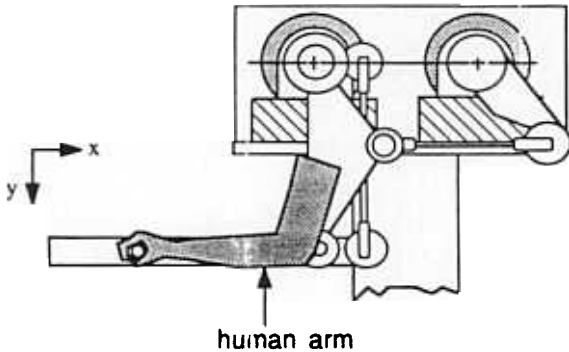


Figure 3: The experimental set-up: the robot is commanded to move sinusoidally, while the human operator grasps the robot handle and attempts to maintain a zero contact force between his hand and the handle.

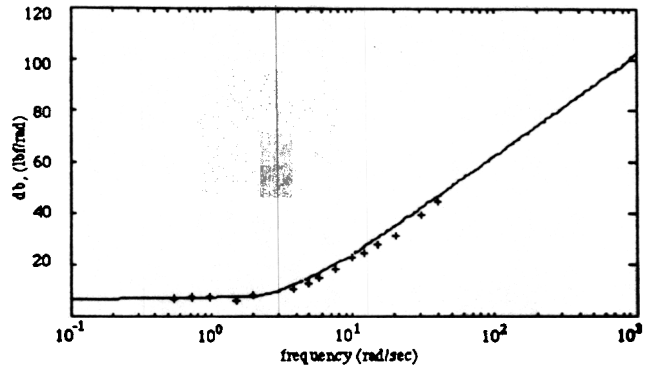


Figure 4: The experimental and theoretical plot of the impedance, G_i , of the human arm at the elbow joint; the operator is maintaining a loose grip on the robot (low co-contraction levels).

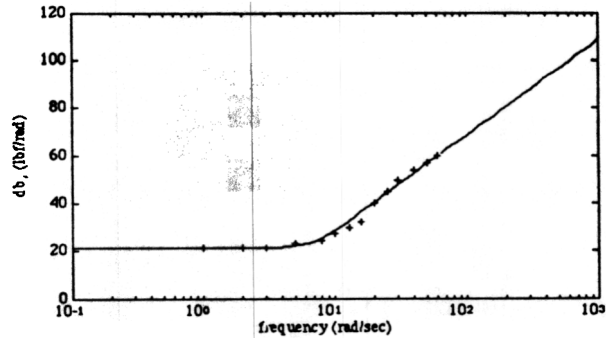


Figure 5: The experimental and theoretical plot of the impedance, G_i , of the human arm at the elbow joint; the operator is maintaining a tight grip on the robot (high co-contraction levels).

4. DISCUSSION AND CONCLUSION

The experimental results discussed here represent preliminary evidence in favor of the model's predictions of arm impedance at varying co-contraction levels and frequencies, when the position of the arm is constrained by the arm's environment.

At very high frequencies, the neural feedback loop is opened, as neural conduction velocities are too slow to allow the body to employ corrective measures based on afferent neural information. The high frequency impedance between the applied position constraint and the contact force represents a measure of the model's performance without the aid of voluntary feedback information. The experimental data regarding the arm impedance support our model's predictions: Since the human arm cannot keep up with the high frequency motion of the robot, the arm's mass dominates its dynamic behavior. The contact force is equal to the product of the robot acceleration and the human arm inertia, by a direct application of Newton's Second Law, and a second order transfer function is expected for the impedance at high frequencies. Consequently, a large

impedance, resulting in large contact forces, is expected at high frequencies.

At very low frequencies, the neural feedback loop is closed, and the arm impedance approximates a constant value that depends upon experimental parameters. In this region, we expect much less agreement between experimental results and model predictions than we expect in the high frequency region, because the value of the impedance depends upon feedback and muscle parameters as well as muscular co-contraction levels. The effect of these parameters is more difficult to quantify than that of the arm inertia, the significant parameter at high frequencies. The predicted impedance of the arm, in the low frequency region, can only be given as a bounded range of impedances. At low enough frequencies, the human can follow the imposed motion comfortably, and he can always establish approximately constant contact forces between his hand and the environment, resulting in a constant impedance when contact forces are small. Although the value of this impedance increases with increasing muscular co-contraction, it remains essentially constant throughout the low frequency region, once a given level of co-contraction has been established.

5. REFERENCES

- Agarwal, G. C., Berman, B. M., and Stark, L. (1970) Studies in postural control systems. Part I. Torque disturbance input. *IEEE Trans. Systems Science Cybernetics* 6, 116-121.
- Berthoz, J. A. and Metral, S. (1970) Behavior of a muscular group subjected to a sinusoidal and trapezoidal variation in force. *J. Appl. Physiol.* 29, 378-384.
- Hayes, K. C. and Hatze, H. (1977) Passive visco-elastic properties of the structures spanning the human elbow joint. *Eur. J. Appl. Physiol.* 37, 265-274.
- Hill, A. V. (1970) *First and last experiments in muscle mechanics*, pp. 23-41, 124-129. Cambridge Univ. Press.
- Humphrey, D. R. and Reed, D. J. (1983) Separate cortical systems for the control of joint movement and joint stiffness: reciprocal activation and coactivation of antagonist muscles. *Adv. Neurology* 39, 347-372.
- Kazerooni, H. (1990) Human-Robot Interaction via the Transfer of Power and Information Signals. *IEEE Trans. on Systems and Cybernetics*, Vol. 20, No. 2, 450-463.
- Kazerooni, H., Mahoney, S. (1991) Dynamics and Control of Robotic Systems Worn By Humans, *ASME Journal of Dynamic Systems, Measurement, and Control*. Vol. 113, No. 3, September 379-387.
- Lehman, S. L. and Calhoun, B. M. (1990) An identified model for human wrist movements. *Exper. Brain Res.* 81, 199-208.
- Murray, W. R. and Hogan, N. (1989) Experimental observations on the maintenance of elbow posture in the presence of disturbances. *Issues in The Modeling and Control of Biomechanical Systems* (Edited by J. L. Stein, J. A. Ashton-Miller, M. G. Pandey), pp. 19-28. ASME.
- Rack, P. M. and Westbury, D. R. (1984) Elastic properties of the cat soleus tendon and their functional importance. *J. Physiol.* 347, 479-495.
- Senturia, S. D. and Wedlock, B. D. (1975) *Electronic Circuits and Applications*, pp. 51-58. John Wiley & Sons, Inc.
- Wieneke, G. H. and Denier van der Gon, J. J. (1974) Variations in the output impedance of the human motor system. *Kybernetik* 15, 159-178.
- Wilkie, D. R. (1950) The relation between force and velocity in human muscle. *J. Physiol.* K110, 248-280.
- Winters, J. M. and Stark, L. (1985) Analysis of fundamental human movement patterns through the use on in-depth antagonistic muscle models. *IEEE Trans. on Biomed. Engr.* BME32, 10, 826-839.
- Winters, J. M. (1990) Hill-based muscle models: a systems engineering perspective. *Multiple Muscle Systems: Biomechanics and Movement Organization* (Edited by J. M. Winters and S. L-Y. Woo), pp. 69-93. Springer Verlag, NY.
- Zahalak, G. I. (1990) Modeling muscle mechanics (and energetics). *Multiple Muscle Systems: Biomechanics and Movement Organization* (Edited by J. M. Winters and S. L-Y. Woo), pp. 1-23. Springer Verlag, NY.
- Zajac, F. (1989) Muscle and tendon: properties, models, scaling and application to biomechanics and motor control. *CRC Crit. Rev. in Biomed. Engr.* 17, 359-415.